Applied Catalysis B: Environmental 160–161 (2014) 582–588

Applied Catalysis B: Environmental

journal homepage: www.elsevier.com/locate/apcatb

Critical influence of surface nitrogen species on the activity of N-doped TiO_2 thin-films during photodegradation of stearic acid under UV light irradiation

Raul Quesada-Cabrera *, Carlos Sotelo-Vazquez, Jawwad A. Darr, Ivan P. Parkin **

University College London, Department of Chemistry, Christopher-Ingold Laboratories, 20 Gordon Street, London WC1H 0AJ, United Kingdom

ARTICLE INFO

Article history:
Received 1 May 2014
Received in revised form 4 June 2014
Accepted 6 June 2014
Available online 16 June 2014

Keywords:
Nitrogen-doped TiO_2
Chemical vapour deposition (CVD)
Thin-films
Photocatalysis
Stearic acid

ABSTRACT

Atmospheric-pressure chemical vapour deposition (APCVD) was used to produce a series of nitrogen-doped titania (N-TiO_2) thin-films using *tert*-butylamine as the nitrogen source. The films were deposited as the anatase phase on glass and quartz substrates and characterised using X-ray diffraction, optical and vibrational spectroscopy and electron microscopy. The nature and location of the nitrogen species present on the surface and bulk of the films was studied by X-ray photoelectron spectroscopy. Thorough comparison amongst films with similar structural and morphological features allowed the role of nitrogen species to be evaluated during photo-oxidation of a model organic pollutant (stearic acid). Sequential photocatalytic experiments revealed a drastic decrease in the UV activity of the films which were correlated with changes involving surface nitrogen groups. The existence of concomitant nitrogen species with similar binding energies (*ca.* 400 eV) but different chemical nature is proposed, as well as the direct participation of at least one of these species in the oxidation reaction. A similar mechanism for the visible light activity of N-TiO_2 materials is also suggested.

1. Introduction

The strategy of doping titania (TiO_2) using non-metal impurities in order to extend the photocatalytic efficiency of the semiconductor to include the visible range is one of the key challenges of photocatalysis. The prolific work reported by Asahi et al. [1] in which nitrogen doping was identified as a promising approach for an effective bandgap narrowing of TiO_2 has spawned active discussion and controversy in the last decade [2–6]. For the most part, the discussion around nitrogen-doped TiO_2 materials (henceforth N-TiO_2) has been focused on their visible light activity and its origins. Many authors have attributed the visible light activity as being due to localised N-2p midgap energy states in the band structure of TiO_2 upon substitution of O^{2-} by N^{3-} (substitutional N_s) species in the TiO_2 lattice [7]. Using X-ray photoelectron spectroscopy (XPS), the presence of N_s species in N-TiO_2 materials is widely assigned to binding energy peaks at *ca.* 397 eV in the N 1s environment. Some authors have suggested that the visible light activity is only indirectly related to the incorporation of substitutional nitrogen N_s in the structure, but rather due to an optimum number of oxygen vacancies (V_{oS}) inherently formed in the doping process [4,7].

The confusion around the photocatalytic efficiency of N-TiO_2 materials has possibly occurred by the often questionable test methods used to assess visible light activity. For example, the photo-oxidation or photo-reduction of dye molecules under irradiation conditions can involve the direct participation of the dye in the reaction (dye-sensitised processes). However, many authors have claimed visible light activity during photodegradation of organic pollutants [1,8–10]. In the latter case, the main hurdle is in the design or setup of the experiment itself, the use of appropriate cut-off filters (even in the case of monochromated light that may include secondary bands at half-wavelength in the UV range), the control of any potential thermal degradation of the target organic pollutant, etc. In addition, many studies have involved photocatalysts with very different physical properties (crystallinity, morphology, surface area, etc.), undetermined ratios of TiO_2 polymorphs, etc., which hinder an appropriate comparison between the efficiencies of doped and undoped compounds. Likewise, the actual incorporation (*doping*) of nitrogen in the material can often be disputed, particularly in works involving the post-treatment of TiO_2 compounds.

In most cases, visible light activity in photocatalysts has been observed to the detriment of UV light activity and a possible

* Corresponding author.
** Corresponding author. Tel.: +44 (0) 20 7679 4669.
E-mail address: r.quesada@ucl.ac.uk (R. Quesada-Cabrera).

http://dx.doi.org/10.1016/j.apcatb.2014.06.010

existence of two opposing mechanisms has been suggested [4]. The presence of N species in interstitial positions (interstitial N_i) in the TiO_2 lattice has been proposed in the case of *enhanced* UV light activity of some N-TiO_2 materials [11]. It is generally accepted that the interstitial nitrogen atoms occupy positions as neutral species (N^0) in the bulk of the TiO_2 lattice. Nevertheless, the nature of these N_i species, with binding energy at *ca.* 400 eV, remains unclear and other species, such as chemisorbed molecular nitrogen (γ-N_2) and NH_x groups have been suggested [4,12].

In the current work, further insight is provided into the origin of the enhanced UV activity, as well as the nature and role of N_i species in N-TiO_2 materials. N-TiO_2 thin-films were synthesised using atmospheric-pressure chemical vapour deposition (APCVD) and their photoactivity was evaluated during photodegradation of octadecanoic (stearic) acid, a model organic pollutant. The deactivation of these materials upon UV cleaning and after sequential stearic acid tests and its correlation with chemical changes involving surface N species suggest the direct participation of surface N groups in the enhanced UV activity observed for some N-TiO_2 materials.

2. Experimental

2.1. Chemical vapour deposition apparatus and film synthesis

All components of the CVD apparatus including gas lines and CVD reactor were kept at high temperature. The precursors were heated independently in stainless steel bubblers and the vapour generated was carried into stainless steel mixing chambers at 250 °C using pre-heated nitrogen gas (*BOC*). Plain nitrogen (N_2) flow carried the mixture of gas precursors through a triple baffle manifold into the reactor. The CVD reactor consisted of a 320 mm-long graphite block contained in a quartz tube, which was heated by three *Whatman* heater cartridges. Pt–Rh thermocouples were used to control the temperature of the individual components of the CVD rig.

All chemicals used in this work were purchased from *Sigma–Aldrich*. Titanium chloride ($TiCl_4$, 99.9%), ethyl acetate ($C_4H_8O_2$, 99%) and *tert*-butylamine ($C_4H_{11}N$, 99.5%) were used as titanium, oxygen and nitrogen sources, respectively. In a typical deposition, the bubbler temperatures of Ti, O and N sources were constant at 340, 310 and 278 K, respectively. The latter temperature was set using an ice bath. The corresponding mass flow rates of Ti and O sources were also constant, 6.7×10^{-3} and 3.1×10^{-3} g min^{-1}, respectively. The flow rates of the N source are indicated in Table 1. The films were deposited at 773 K, either on quartz slides (25 mm × 25 mm × 4 mm, *Multi-Lab*) or float glass substrates (89 mm × 225 mm × 4 mm, supplied from *Pilkington NSG Group*). The glass substrates were fabricated with a silica (SiO_2) barrier layer to prevent ion diffusion into the film. The substrates were thoroughly cleaned using acetone (C_3H_6O, 99%), isopropanol (C_3H_8O, 99.9%) and distilled water and dried in air prior to use.

2.2. Analytical methods

X-ray diffraction (XRD) studies were performed using a Bruker-Axs D8 (GADDS) diffractometer equipped with a monochromated ($K\alpha_1$ and $K\alpha_2$) Cu X-ray source and a 2D area X-ray detector with a resolution of 0.01°. The films were analysed with a glancing incident angle (θ) of 5°. The diffraction patterns obtained were compared with database standards. Raman spectroscopy was carried out using a Renishaw 1000 spectrometer equipped with a 514 nm laser. The Raman system was calibrated using a silicon reference. Absorption spectroscopy was performed using a double beam, double monochromated Perkin Elmer Lambda 950 UV/vis/NIR Spectrophotometer. The absorption spectra were recorded directly on the films as deposited on quartz slides, clamped against an integrating sphere in perpendicular position to the beam path. A Labsphere reflectance standard was used as reference in the UV/vis measurements. The thickness of the films was typically estimated using the *Swanepoel* method [13] using reflectance spectra in the range 300–2500 nm, recorded on a Helios double beam instrument standardised relative to a silicon mirror. The estimated thickness of selected films was confirmed using side-view scanning electron microscopy (SEM). SEM analysis was carried out using secondary electron image on a JEOL 6301 field-emission instrument (5 kV). X-ray photoelectron spectroscopy (XPS) was performed using a *Thermo Scientific*™ K-alpha™ spectrometer, with monochromated Al Kα radiation, a dual beam charge compensation system and constant pass energy of 50 eV. Survey scans were collected in the energy range of 0–1200 eV. High-resolution peaks were used for the principal peaks Ti (2p), O (1s), N (1s), C (1s) and Si (2p). The peaks were modelled using sensitivity factors to calculate the film composition. The area underneath these bands is an indication of the concentration of element within the region of analysis (spot size 400 μm).

2.3. Photocatalytic test and irradiation conditions

The photodegradation of stearic acid was monitored *via* Fourier transform infrared (FTIR) spectroscopy in the range 2700–3000 cm^{-1}, using a Perkin Elmer RX-I instrument. A thin film of stearic acid was dip-coated onto the photocatalytic films from a 0.05 M stearic acid solution in chloroform. The IR spectra were collected in absorbance mode and the integrated areas of typical C—H bands of the acid at 2958, 2923 and 2853 cm^{-1} monitored upon illumination (Fig. 1). These bands give an estimation of the number of molecules of stearic acid degraded using a conversion factor reported in the literature (1 cm^{-1} ≡ 9.7×10^{15} mol) [14]. The photoactivity rates were estimated from linear regression of the initial 30–40% degradation steps (zero-order kinetics). These rates may be

Table 1
Film description and experimental details for the deposition of undoped (Ti1) and N-doped TiO_2 (NTi-) films. The temperature and mass flow conditions were constant for metal ($TiCl_4$) and oxygen ($C_4H_8O_2$) precursors: 340 and 310 K, and 6.7×10^{-3} and 3.1×10^{-3} g min^{-1}, respectively.

Sample	Mass flow N source × 10^{-3} (g min^{-1})	Growth rate (nm min^{-1})	R_0 (cm^{-1} h^{-1})	FQE × 10^{-4} (mol photon^{-1})
Ti1	–	355	0.078	0.92
NTi1	1.262	390	0.195	2.30
NTi2	0.643	360	0.105	1.24
NTi3	0.598	410	0.094	1.11
NTi4	0.561	335	0.083	0.98
NTi4/UV	–	–	0.029	0.34
NTi4/H_2O	–	–	0.047	0.56
NTi5	1.338	330	0.218	2.77
NTi5′	–	–	0.103	1.30
NTi5″	–	–	0.085	1.08

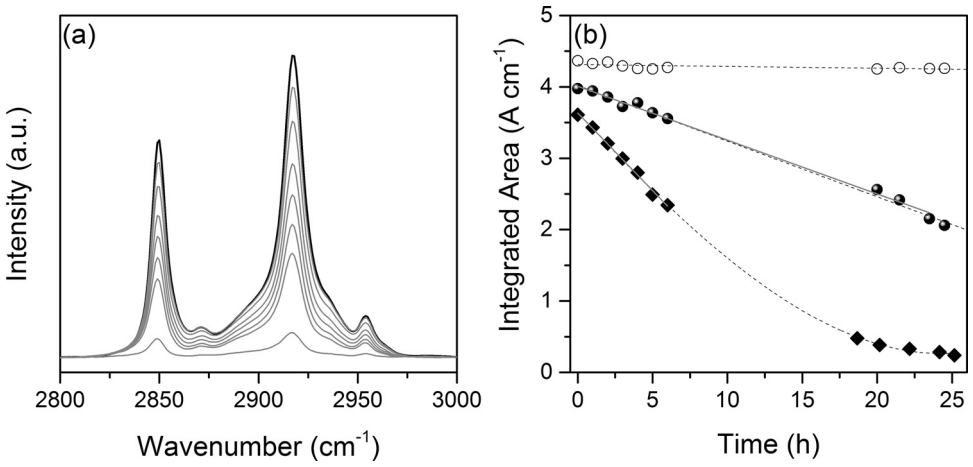

Fig. 1. (a) Typical IR spectra collected during the photodegradation of stearic acid on a N-TiO_2 film over 25 h. (b) Integrated areas of stearic acid bands estimated during UVA illumination of undoped (full circles) and N-doped (full diamonds) TiO_2 films. The areas obtained from the acid on plain glass are included for reference (empty circles). The corresponding photocatalytic rates were calculated from linear regression of the initial 30–40% degradation steps (grey lines).

given as formal quantum efficiency (FQE) values, which are defined as the number of acid molecules degraded per incident photon. The overall degradation reaction is:

$$CH_3(CH_2)_{16}CO_2H + 26O_2 \xrightarrow{TiO_2(h\nu \geq E_{bg})} 18CO_2 + 18H_2O \quad (1)$$

A blacklight-bulb (BLB) UVA lamp (*Vilber-Lourmat*), 2 × 8 W, was used in the photocatalytic tests. The irradiance of the UV lamp (1.2 mW cm^{-2}) was measured using a UVX meter (*UVP*). Further visible light tests were carried out using a solar simulator (AM1.5), 75 W Xe lamp (*PTI QuantaMaster*™ *400*), with a cut-off 420 nm filter (*VMI*). The irradiation area of the samples was 0.78 cm^2. The as-deposited films were UV cleaned under wet-air conditions during 24 h and kept in the dark for at least 24 h previous to any photoactivity test.

3. Results and discussion

3.1. Film characterisation

A range of N-TiO_2 thin-films were deposited by APVCD of titanium tetrachloride ($TiCl_4$), ethyl acetate ($C_4H_8O_2$) and *tert*-butylamine ($C_4H_{11}N$) on glass and quartz substrates at 500 °C. The as-deposited films were in the thickness range within 350–420 nm (Table 1). In general, it was observed that the introduction of low N levels (<1 at.%, as determined by XPS) had little or no impact on the physical properties of the doped films compared to undoped samples. These N-TiO_2 films were pure anatase and no traces of rutile, titanium nitride or any other nitrogen-containing structures were detected by XRD and Raman spectroscopy (Fig. 2). The XRD patterns of doped and undoped films showed comparable peak broadening (FWHM ~0.5°), peak intensities and peak area ratios (Fig. 2(a)). Likewise, the surface structure of the films was largely unaffected by the incorporation of low amounts of nitrogen (<1 at.% N). Scanning electron microscopy (SEM) images of undoped TiO_2 films revealed relatively rough surfaces formed by large star-like aggregated particles (Fig. 3(a)) whereas the N-TiO_2 films showed slightly more compacted surface structures with flat particles apparently merged together (Fig. 3(b)). In contrast, the N-TiO_2 films designed to contain relatively high amounts of nitrogen (>1 at.% N) showed poor XRD patterns and Raman spectra (weak and broad peaks), as well as degraded, amorphous-like surface structures in some extreme cases, in line with the observations

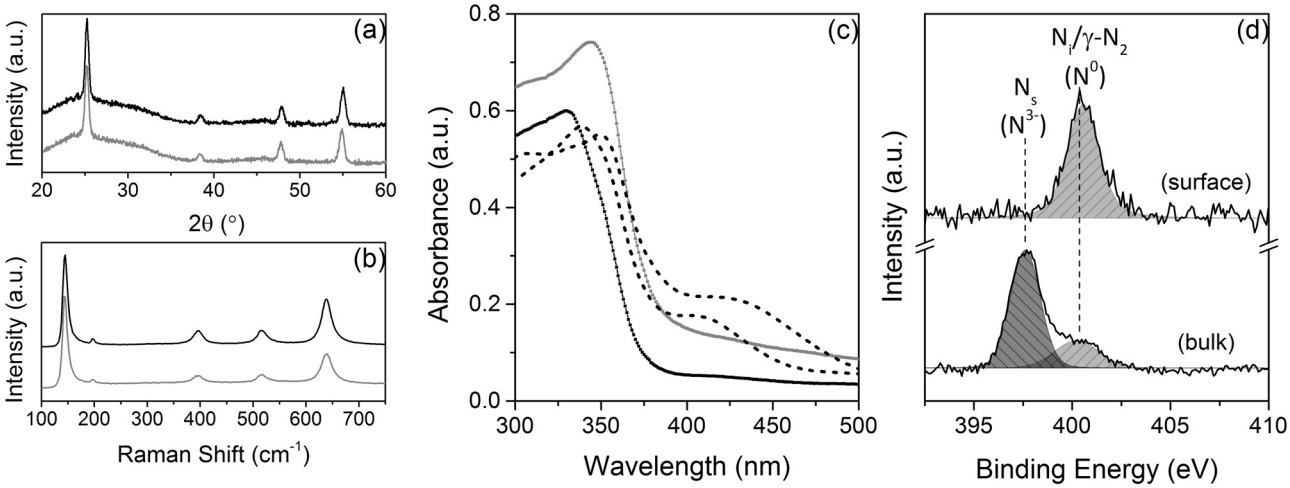

Fig. 2. (a) Typical X-ray diffraction patterns (λ = 1.5406 Å) and (b) Raman spectra of undoped (black line) and N-doped (grey line) TiO_2 thin-films deposited using *tert*-butylamine as nitrogen source (<1 at.% N). These are representative films considered for the photocatalytic assessment. (c) Absorption spectra of typical undoped (black line) and N-doped (grey line) TiO_2 films (~0.5 at.% N) used in the photocatalytic testing. The spectra of N-TiO_2 films containing relatively high N total concentrations (>1 at.% N) have been included for comparison (dashed lines). (d) Typical surface and bulk XPS data from the N 1s environment of an as-deposited N-TiO_2 film. The bulk data represents an average of the spectra collected during Argon sputtering of the film. General assignments of XPS peaks have been included.

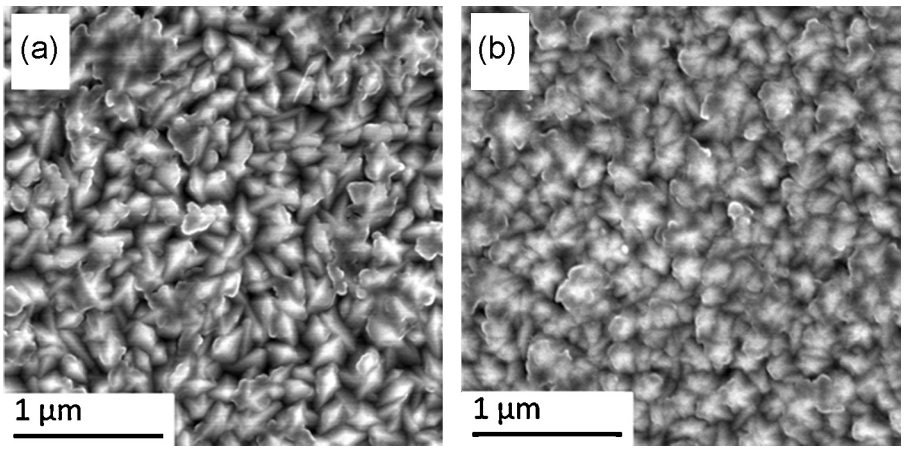

Fig. 3. Scanning electron microscopy (SEM) images (25,000×) of representative undoped (a) and N-doped (b) TiO_2 films as deposited using *tert*-butylamine as nitrogen source.

reported in the literature [7,15,16]. In addition, traces of additional phases, which likely corresponded to oxynitride compounds, were detected in the latter films using Raman spectroscopy. Thus, only N-TiO_2 films which contained low nitrogen levels (<1 at.% N) were considered for the photocatalytic assessment in this work, to allow a fair comparison with similar undoped TiO_2 reference samples.

The undoped TiO_2 films were colourless and translucent, showing an absorption onset at *ca.* 380 nm and maximum absorbance at 330 nm (Fig. 2(c)), whereas the N-TiO_2 films used in the photocatalytic testing were typically yellow and their corresponding absorption edge was red-shifted with respect to that of the undoped films. Some N-TiO_2 films with relatively high content of nitrogen (>1 at.% N) showed additional absorption bands in the range of 400–450 nm, as shown in Fig. 2(c). All of these absorption features are consistent with previous reports [4,7,17–19].

The nature and concentration of N species incorporated in the N-TiO_2 films were studied by XPS and their influence on the photoactivity of these materials is discussed in the following section (*vide infra*). As stated above, nitrogen can be incorporated into the TiO_2 structure in oxygen lattice sites (as N^{3-}, *substitutional* N_s) or in interstitial positions (as N^0, *interstitial* N_i), which are commonly assigned to binding energies of *ca.* 397 and 400 eV, respectively, by XPS analysis [1,4,6,7]. All the as-deposited N-TiO_2 films showed a single binding-energy peak at 400.6 eV (N_i) on the surface and *both* environments (N_i and N_s), *i.e.* different ratios of the peaks at 397.6 and 400.6 eV, in the bulk of the films (Fig. 2(d)). It should be noted that the peak at 400.6 eV on the surface of N-TiO_2 materials has also been widely assigned to chemisorbed nitrogen (γ-N_2), as indicated in the figure. Nevertheless, the latter peak was not observed in the XPS analysis of undoped TiO_2 films, despite the fact that nitrogen (N_2) is used as a carrier gas during the APCVD synthesis. Hence, we do not consider chemisorbed nitrogen as being the progenitor of the 400 eV XPS peak.

3.2. Influence of the nitrogen environment on the photoactivity of N-TiO_2 films

The overall impact of nitrogen doping on the photoactivity of N-TiO_2 films was investigated *via* photodegradation of stearic acid, as described in the experimental section. Comparable undoped (Ti1) and doped TiO_2 films (NTi1, NTi2 and NTi3), which showed similar XRD patterns (Fig. 4(a)), were investigated in the initial photocatalytic tests carried out under UVA illumination (BLB lamp, 1.2 mW cm^{-2}). Bulk average XPS analysis of these films showed very similar N_s levels (397.6 eV) but different concentrations of surface and bulk N_i species (400.6 eV) (Fig. 4(b)). The corresponding UV activities of these films, given as formal quantum efficiencies (units, mol $photon^{-1}$), and relative content of the different N species are

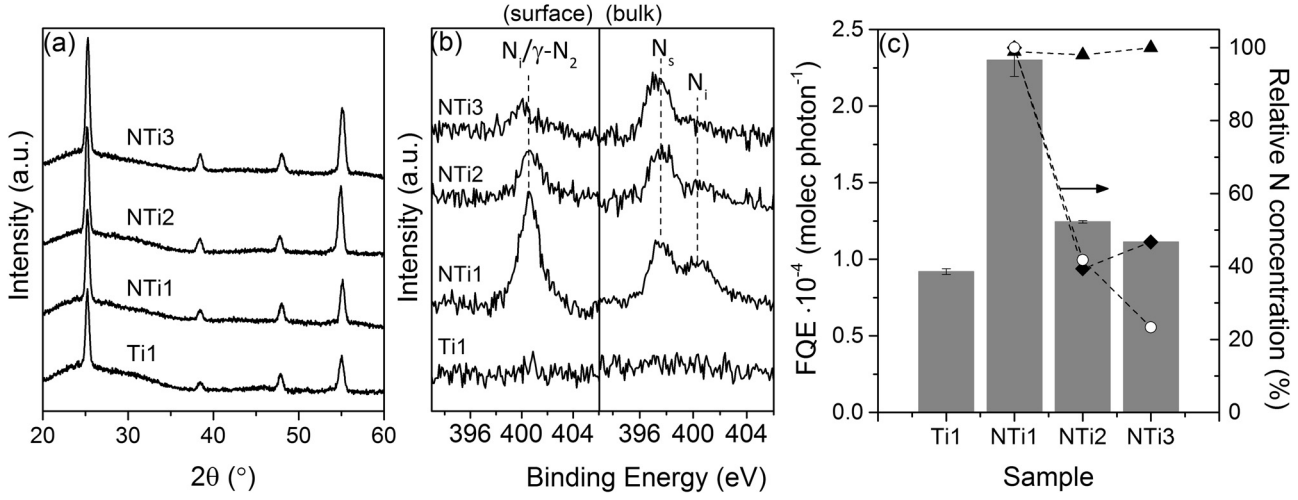

Fig. 4. (a) X-ray diffraction patterns (λ = 1.5406 Å) of selected N-TiO_2 films (NTi1, NTi2 and NTi3) and as-deposited undoped TiO_2 film (Ti1) used as reference. (b) Corresponding XPS spectra of surface (left) and bulk average (right) species in the N 1s environment (assignments included). (c) Respective formal quantum efficiencies. The relative levels (%) of surface (empty circles), interstitial (full diamonds) and substitutional (full triangles) nitrogen are indicated for comparison.

indicated in Fig. 4(c). A general increase in activity, compared to the undoped TiO_2 sample (Ti1), was initially observed for the N-TiO_2 films which contained high levels of N_i species (NTi1). In contrast, the activity of N-TiO_2 films with very low N_i levels (NTi3) was comparable to that of the undoped Ti1 film, despite the relatively high content of substitutional N_s species in the former film. Thus, the enhanced UV activity of N-TiO_2 films was attributed to the influence of N_i species alone, in agreement with previous observations by the authors [11]. Indeed, the trend of activities observed for samples NTi1, NTi2 and NTi3 followed the relative concentrations of N_i species estimated from XPS data, as inferred from Fig. 4(c). Further insight into the role of these species in the apparent enhancement of the UV activity of N-TiO_2 films will be discussed in the following section (*vide infra*).

Stearic acid tests were also carried out under visible light irradiation (75 W Xe lamp, AM1.5 and cut-off UV filter) over 3 days, however, no visible activity was detected for any of our N-TiO_2 films beyond instrumental error. Many authors have reported visible light activity during photodegradation of organic pollutants using N-TiO_2 materials and correlation with N species with binding energies of *ca.* 397 eV (N_s) has been suggested [1,8–10]. These species were only found in the bulk of our films together with interstitial N species and it is unclear whether the presence of the latter would have a detrimental effect on the potential visible light activity of the films.

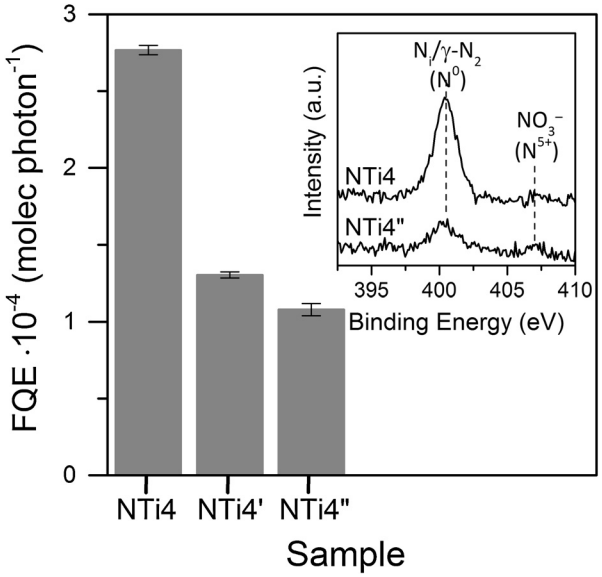

Fig. 5. Formal quantum efficiencies obtained during sequential photodegradation of stearic acid on a N-TiO_2 film under UVA illumination. The labels NTi4, NTi4′ and NTi4″ correspond to a first, second and third test, respectively. The inset shows the corresponding surface XPS spectra (N 1s environment) of the as-deposited film before the stearic acid tests and after the sequential testing. Typical assignments for the N species are included for reference.

3.3. Photostability of N-TiO_2 films

Sequential photoactivity tests were carried out under UVA irradiation in order to investigate the photostability of the N-TiO_2 films. After each test, the sample was washed in pure chloroform under stirring conditions to eliminate any trace of stearic acid and a new layer of acid was deposited for subsequent testing. Surprisingly, it was found that the activity rates progressively dropped (Fig. 5) until reaching a minimum value, which corresponded to those expected for comparable undoped TiO_2 films. XPS analysis of the surface of the N-TiO_2 film (NTi4) after sequential tests showed a concomitant decrease in area of the peak at 400.6 eV (N_i) and a weak new peak at 407.6 eV. The latter has been assigned to the binding energy of NO_3^- (N^{5+}) species [20].

Insight into the nature of the binding-energy peak at 400.6 eV on the surface of N-TiO_2 films and its role in the apparent photoactivity of these materials were further investigated upon UV *cleaning* of the films. UVA (or UVC) irradiation of synthesised photocatalysts is common practise to clean the surface of the materials of residual organic contaminants. However, we found that UVA cleaning of the as-deposited N-TiO_2 films under high humidity (wet-air) conditions caused important changes on the surface N species, as detected by XPS. Fig. 6(a) illustrates the effect of UVA illumination (1.2 mW cm^{-2}) on a typical N-TiO_2 film (NTi5). It can be observed that, after irradiation for 48 h, the initial surface peak at 400.6 eV (N_i) decreased to approximately half of the initial area (NTi5/UV) and a new XPS peak at 407.6 eV (NO_3^-) appeared. This observation suggests that the partial photo-oxidation of the N species with binding energy of 400.6 eV resulted in the formation of NO_3^- groups on the surface of the film. These chemical changes had a detrimental effect on the photocatalytic performance of the film (Fig. 6(b)), as

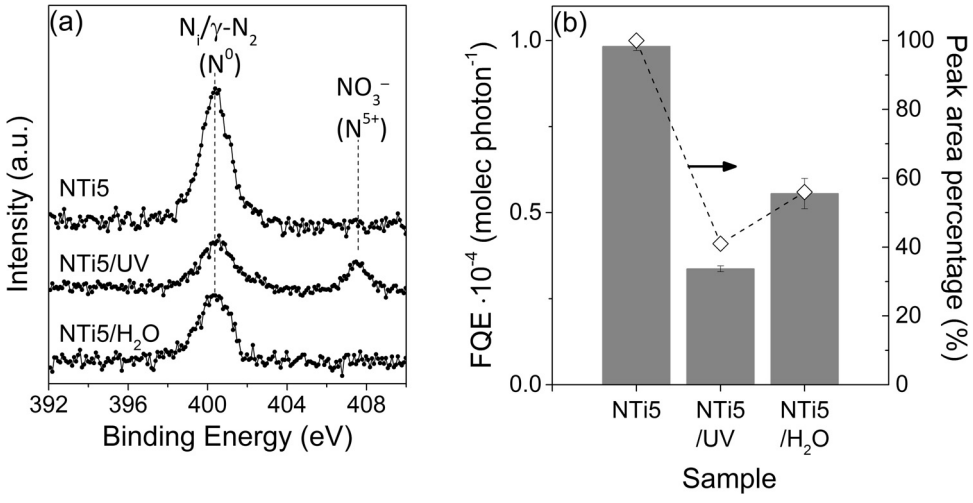

Fig. 6. (a) XPS surface spectra in the N 1s environment of a typical as-deposited N-TiO_2 film (NTi5) after UVA *cleaning* (48 h, BLB lamp, 1.2 mW cm^{-2}) (NTi5/UV) and subsequent washing in DI water (NTi5/H_2O). The assignments indicated are widely accepted for N species with binding energies at *ca.* 400 (N_i/γ-N_2) and 407.6 eV (NO_3^-). (b) Corresponding change in UV photoactivity during degradation of stearic acid under identical irradiation conditions after each of the steps shown in the XPS data (deposition, UV cleaning and washing).

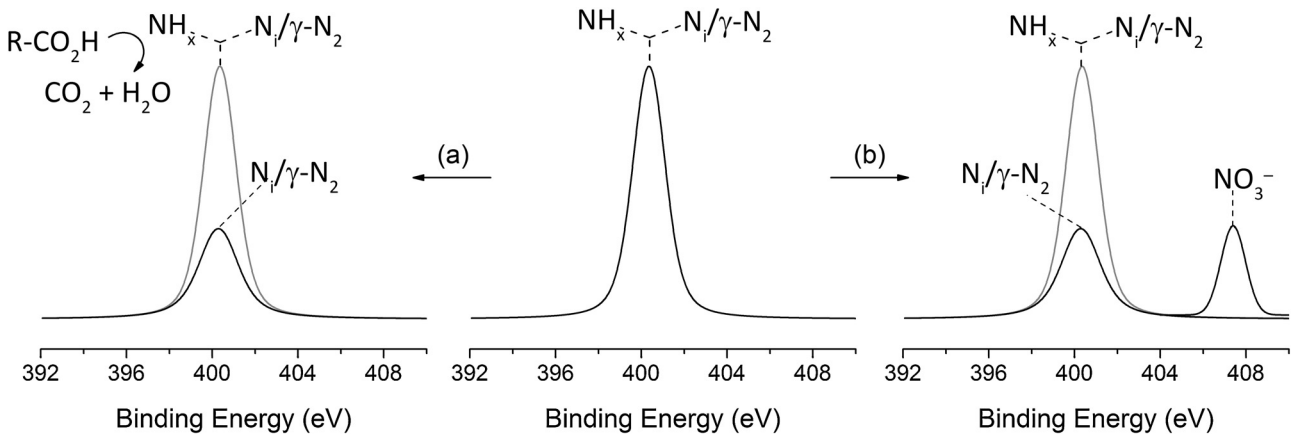

Fig. 7. Schematic figure illustrating the proposed reactions of surface nitrogen species with binding energy at *ca.* 400 eV. The central XPS peak could be originated from concomitant N species such as (inactive) N_i/γ-N_2 and (active) NH_x groups. (a) The mineralisation of an organic pollutant may be intermediated by highly oxidating species (N—O radicals) formed during photo-oxidation of NH_x species. (b) In the absence of organic molecules, these radicals may readily form salt (NO_3^-) groups, as observed in this work. In both cases, (a) and (b), the remaining peak at 400 eV after the respective reactions is probably due to the inactive N_i/γ-N_2 species.

expected, since the nitrate groups may be formed on active sites and thus poison the photocatalyst surface. Nevertheless, it was relevant to observe that the photoactivity rates remained low after washing the film in DI water (NTi5/H_2O), despite the fact that the NO_3^- groups have been removed from the film surface (Fig. 6(a)). Significantly, the photoactivity of the washed NTi5/H_2O film correlated with the decrease in area of the binding-energy peak at 400.6 eV on the surface of the photocatalyst, which suggest a *direct* influence of adsorbed N_i species on the oxidation reaction mechanism of stearic acid.

It was also important to notice that the nitrogen species on the surface of the N-TiO_2 film were not completely converted to NO_3^- even after prolonged UVA irradiation (*ca.* 7 days) and the peak at 400.6 eV seemed to reach a minimum after which no chemical changes were observed by XPS analysis. However, once the peak at 400.6 eV reached this minimum, the activity of the N-TiO_2 film was comparable to that of similar undoped TiO_2 films. This could be explained assuming the concomitant presence of N species with similar binding energies (*ca.* 400 eV) but different chemical nature. Yates et al. [12] suggested interstitially bound NH_x species with binding energies at *ca.* 400 eV as the active dopant in silver deposition experiments. The photo-oxidation of NH_x species could lead to formation of •NO radicals and highly oxidising species, including products of the reaction with superoxide ($O_2^{\bullet -}$) and hydroxyl radical groups, which may participate in the oxidation reaction of organic molecules (Fig. 7(a)). In the absence of an organic pollutant, these species could also be readily oxidised into NO_3^- groups, as observed after UV cleaning of the N-TiO_2 films (Fig. 7(b)), while unreactive N_i/N_2 groups (also at *ca.* 400 eV) would remain on the surface even after prolonged UV irradiation. Thus, the apparent enhanced UV photoactivity of N-TiO_2 materials would only be effective for as long as active NH_x species are present on the surface of the photocatalyst.

Interestingly, photo-induced deactivation of N-TiO_2 compounds has also been reported during visible light irradiation. Nosaka et al. [8] observed that the activity of their N-TiO_2 materials decreased to one half of the initial rate during degradation of 2-propanol after prolonged visible light illumination (100 h) using a 500 W super high-pressure Hg lamp with a glass UV filter. Consistent with our observations, these authors also observed a concomitant decrease of the main XPS peak in the N 1s environment. It is therefore possible that surface N species would have a role in the reported visible-light-driven reactions involving N-TiO_2 materials in the literature.

4. Conclusions

N-TiO_2 thin-films were synthesised using atmospheric-pressure chemical vapour deposition. The films were deposited as single-phase anatase and contained different ratios of interstitial (N_i) and substitutional (N_s) nitrogen species, as evidenced by XPS depth profiling, with binding energies at 400.6 and 397.6 eV, respectively. The surface N species identified showed binding energies at *ca.* 400 eV, typically assigned to interstitial N_i and chemisorbed molecular nitrogen (γ-N_2). However, the latter was not observed in the undoped TiO_2 samples, despite the use of nitrogen as carrier gas in the deposition of the films.

The as-deposited N-TiO_2 films showed enhanced UV activities compared to those of similar undoped TiO_2 samples, which were correlated with levels of interstitial N species at 400 eV. Nevertheless, a decrease in UV-photoactivity was observed after sequential stearic acid tests and also after UV cleaning of the doped films. These observations were related to a concomitant decrease in the XPS peak at 400 eV. Once this peak reached a minimum, the activity of the N-TiO_2 film was similar to that of a comparable undoped sample.

It was concluded that the surface XPS peak at *ca.* 400 eV was due to the presence of concomitant N species, in agreement with some literature reports. Direct participation of active N groups (likely NH_x species) in the photodegradation reaction mechanism was proposed, likely involving highly oxidising N—O radicals. These active species would form nitrate (NO_3^-) groups in the absence of an organic pollutant, as observed in this work. At the same time, inactive interstitial nitrogen N_i groups are assigned for the peak at 400 eV, which remains after the degradation reaction.

No visible light activity was observed for any of the films investigated in this work. However, the deactivation of N-TiO_2 materials reported by some authors suggests that surface N species could be responsible for the apparent visible light activity claimed in some cases in the literature.

Acknowledgements

European Commission FP7 is thanked for funding (PCATDES, Grant No. 309846). Dr. Robert Palgrave is thanked for his assistance in the XPS analysis and Kevin Reeves for assistance with the SEM instrument.

References

[1] R. Asahi, T. Morikawa, T. Ohwaki, K. Aoki, Y. Taga, Science 293 (2001) 269–271.
[2] R. Asahi, T. Morikawa, Chem. Phys. 339 (2007) 57–63.
[3] R. Asahi, T. Morikawa, H. Hazama, M. Matsubara, J. Phys.: Condens. Matter 20 (2008) 064227–064233.
[4] A.V. Emeline, V.N. Kuznetsov, V.K. Rybchuk, N. Serpone, Int. J. Photoenergy 2008 (2008) ID258394–ID258413.
[5] J. Zhang, Y. Wu, M. Xing, S.A.K. Leghari, S. Sajjad, Energy Environ. Sci. 3 (2010) 715–726.
[6] B. Viswanathan, K.R. Krishanmurthy, Int. J. Photoenergy 2012 (2012) ID269654–ID269663.
[7] M. Batzill, E.H. Morales, U. Diebold, Phys. Rev. Lett. 96 (2006) 026103-1–026103-4.
[8] Y. Nosaka, M. Matsushita, J. Nishino, A.Y. Nosaka, Sci. Technol. Adv. Mater. 6 (2005) 143–148.
[9] M. Maeda, T. Watanabe, J. Electrochem. Soc. 153 (2006) C186–C189.
[10] M. Miyauchi, A. Ikezawa, H. Tobimatsu, H. Irie, K. Hashimoto, Phys. Chem. Chem. Phys. 6 (2004) 865–870.
[11] A. Kafizas, C. Crick, I.P. Parkin, J. Photochem. Photobiol. A: Chem. 216 (2010) 156–166.
[12] O. Diwald, T.L. Thompson, T. Zubkov, E.G. Goralski, S.D. Walck, J.T. Yates, J. Phys. Chem. B 108 (2004) 6004–6008.
[13] R. Swanepoel, J. Phys. E: Sci. Instrum. 16 (1983) 1215–1217.
[14] A. Mills, J.S. Wang, J. Photochem. Photobiol. A: Chem. 182 (2006) 181–186.
[15] U. Diebold, Surf. Sci. Rep. 48 (2003) 53–229.
[16] H.M. Yates, M.G. Nolan, D.W. Sheel, M.E. Pemble, J. Photochem. Photobiol. A: Chem. 179 (2006) 213–223.
[17] V.N. Kuznetsov, N. Serpone, J. Phys. Chem. C 113 (2009) 15110–15123.
[18] T. Morikawa, R. Asahi, T. Ohwaki, K. Aoki, Y. Taga, Jpn. J. Appl. Phys. 40 (2001) L561–L563.
[19] P.-G. Wu, C.-H. Ma, J.K. Shang, Appl. Phys. A 81 (2005) 1411–1417.
[20] J.A. Rodriguez, T. Jirsak, G. Liu, J. Hrbek, J. Dvorak, A. Maiti, J. Am. Chem. Soc. 123 (2001) 9597–9605.